

Determination of $E_2^\circ - E_1^\circ$ in Multistep Charge Transfer by Stationary-Electrode Pulse and Cyclic Voltammetry: Application to Binuclear Ruthenium Amines

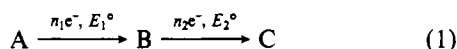
DAVID E. RICHARDSON and HENRY TAUBE*

Received May 20, 1980

The techniques of pulse and cyclic voltammetry have been applied to the determination of $E_2^\circ - E_1^\circ$ for two-step electrochemical charge transfers. A simple theory has been derived for the dependence of the differential-pulse response on E_1° , E_2° , and the pulse amplitude. A previously published width method for determining $E_2^\circ - E_1^\circ$ from cyclic voltammograms has been extended to any value of ΔE° . The use of the peak-to-peak separation in cyclic voltammetry has also been evaluated. Working curves are presented to allow simple graphical conversion of experimental data to ΔE° . The two techniques are tested with a series of binuclear ruthenium complexes having values of ΔE° from about 50 to 150 mV. Comparison with a spectrophotometric titration method shows agreement of comproportionation constants within 10%. Overall fit of theory to experiment is good for both methods, but the differential-pulse method is preferred for experimental reasons.

Introduction

Many substances can undergo multistep charge-transfer reactions of the type

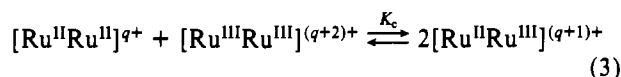


The relation of the concentrations of A and C to B at equilibrium is expressed by the comproportionation constant, K_c , where

$$K_c = \frac{[B]^{n_1+n_2}}{[C]^{n_1}[A]^{n_2}} = \exp \left[\frac{(E_1^\circ - E_2^\circ)n_1 n_2 F}{RT} \right] \quad (2)$$

When $n_1 = n_2 = 1$, $K_c = \exp(\Delta E^\circ/25.69)$ at 298 K, with ΔE° given in mV. Symbols are defined in Appendix I.

In our study^{1,2a} of binuclear complexes of ruthenium it became necessary to determine K_c for the reaction



(where $\text{Ru}^{\text{II}}\text{Ru}^{\text{II}}$ etc. represent the discrete binuclear complexes of the general type $[(\text{NH}_3)_5\text{Ru}-\text{L}-\text{Ru}(\text{NH}_3)_5]$ for systems in which K_c is not much larger than the statistical value. Such determinations by a spectrophotometric titration have been reported recently² by Sutton et al. With that method, values of K_c accurate to $\pm 5\%$ are obtainable in the range $4 < K_c < \text{ca. } 200$ ($36 \text{ mV} < \Delta E^\circ < 136 \text{ mV}$). However, the success of the spectrophotometric titration requires that rather stringent conditions be met. All species involved in equilibrium 3 must be soluble and stable over the time required for an accurate titration (~ 30 – 60 min), and there must be an isolated absorption band characteristic of a single species. Sutton et al.² used the near-infrared intervalence-transfer band of the mixed-valence species $[\text{Ru}^{\text{II}}\text{Ru}^{\text{III}}]$.³ Unfortunately, the strategy they used is not always applicable. For many complexes we have studied, the intervalence band is weak ($\epsilon < 50 \text{ M}^{-1} \text{ cm}^{-1}$) and appears on the shoulder of an intense visible charge-transfer band. Furthermore, side reactions of the II,III

and III,III species vitiate the titration method because of the time required for titration.

In many cases, ΔE° can be estimated from $\Delta E_{1/2}$ obtained by electrochemical methods. The standard potential is related to $E_{1/2}$ by the equation⁴

$$E^\circ = E_{1/2} - \left(\frac{RT}{nF} \right) \ln \left(\frac{D_R}{D_O} \right)^{1/2} \left(\frac{f_O}{f_R} \right) \quad (4)$$

(See Appendix I for definition of symbols.) If the diffusion coefficients are roughly equal, the second term on the right side of eq 4 is small, at least in the absence of effects which make f_O and f_R widely different, and $E^\circ \approx E_{1/2}$. For example, a 10% difference in D_O and D_R yields a value of about 3 mV for the second term if $f_O/f_R = 1$.

Typically, cyclic voltammetry has been used to obtain $\Delta E_{1/2}$.⁵ A theory of two-step cyclic voltammetry at stationary electrodes has been given by Polcyn and Shain.⁶ Their results show that when $\Delta E_{1/2}$ is less than about 120 mV, the two separate peaks are not resolved. Myers and Shain⁷ have given a working curve applicable to the region $-80 \text{ mV} < \Delta E_{1/2} < 50 \text{ mV}$ for the width of a multistep response, $(E_p - E_{p/2})$ vs. $\Delta E_{1/2}$. They did not extend the working curve beyond $\Delta E_{1/2} = 50 \text{ mV}$ since the wave becomes distorted at that point. For $n_1 = n_2 = 1$, this would appear to limit their method to $K_c \leq 7$. We will show, however, that their method can be extended to any value of $\Delta E_{1/2}$.

Electrochemical techniques have several advantages over the spectrophotometric method described earlier. They can be applied over the whole experimentally accessible range of $\Delta E_{1/2}$ values,⁵ and rapid techniques can be chosen to accommodate the stabilities of the species involved. Only small amounts of material are required ($< 1 \text{ mg}$). Working curves⁸ can be constructed to eliminate the need for simulation of current-potential response for each experiment (the spectrophotometric method² requires a computer-fitting routine to analyze the experimental data). Theories are available to deal with cases where one (or both) of the charge-transfer steps

(1) (a) Taube, H. *Ann. N.Y. Acad. Sci.* **1978**, *313*, 481. (b) Taube, H. "Tunneling in Biological Systems"; Chance, B., DeVault, D. C., Frauenfelder, H., Schreiffer, J. R., Sutlin, N., Eds.; Academic Press: New York, 1978; p 173.
(2) (a) Sutton, J. E.; Sutton, P. M.; Taube, H. *Inorg. Chem.* **1979**, *18*, 1017. (b) Sutton, J. E. Ph.D. Thesis, Stanford University, 1979.
(3) (a) Hush, N. S. *Prog. Inorg. Chem.* **1967**, *8*, 391. (b) Hush, N. S. *Electrochim. Acta* **1968**, *13*, 1005. (c) Robin, M.; Day, P. *Adv. Inorg. Chem. Radiochem.* **1967**, *10*, 247. (d) Wong, K. Y.; Schatz, P. N.; Piepho, S. B. *J. Am. Chem. Soc.* **1979**, *101*, 2793. (e) Schatz, P. N. "Proceedings of NATO-ASI on Mixed Valence Compounds in Chemistry, Physics and Biology"; Brown, D. B., Ed.; Reidel: Dordrecht, 1980.

(4) Delahay, P. "New Instrumental Methods in Electrochemistry"; Interscience: New York, 1954; p 56.

(5) E.g.: (a) Fenton, D. E.; Schroeder, R. R.; Lintvedt, R. L. *J. Am. Chem. Soc.* **1978**, *100*, 1931. (b) See ref 24 and references cited therein. Differential-pulse voltammetry has also been used. E.g.: (c) Gagne, R. R.; Koval, C. A.; Smith, T. J.; Cimolino, M. C. *J. Am. Chem. Soc.* **1979**, *101*, 4571. (d) Mayerle, J. J.; Denmark, S. E.; DePamphilis, B. V.; Ibers, J. A.; Holm, R. H. *Ibid.* **1975**, *97*, 1032. (e) Isied, S. S.; Kuehn, C. G. *Ibid.* **1978**, *100*, 6754.

(6) Polcyn, D.; Shain, I. *Anal. Chem.* **1966**, *38*, 370, 376.

(7) Myers, R. L.; Shain, I. *Anal. Chem.* **1969**, *41*, 980.

(8) (a) Nicholson, R. S.; Shain, I. *Anal. Chem.* **1964**, *36*, 706. (b) Nicholson, R. S. *Ibid.* **1965**, *37*, 1351.

is irreversible.^{6,9} As in the spectrophotometric titration, impurities will not affect the results if they are electrochemically inactive in the potential region of interest.

The complexity of multistep cyclic voltammetry current-potential curves when $\Delta E_{1/2} < 250$ mV led us to evaluate application of pulse voltammetry to the problem. Normal- and differential-pulse voltammetries at stationary electrodes have been studied by Osteryoung and coworkers.¹⁰ The use of a stationary electrode makes possible the extension of the anodic range well beyond that of the DME (0.3 V vs. SCE in aqueous solvent).^{11a,12} This has proven especially useful for the complexes we have studied, since many of them have half-potentials well outside the range of mercury.

Theory

A general theory of multistep charge transfers at electrodes has been offered by Ruzic,⁹ but we will be concerned only with cases where both charge transfers are reversible and the rate of electron transfer at the electrode surface is sufficient to maintain Nernstian conditions, that is

$$C_{O^\circ} / C_{R^\circ} = \exp[(nF/RT)(E - E_{1/2})] \quad (5)$$

Also, linear diffusion will be assumed in expressions for the current. An unshielded planar electrode closely approximates this condition.^{11b}

Normal Pulse. The theory of normal-pulse voltammetry at stationary electrodes¹³ shows that the same current-potential relationship is obtained as found for dc polarography at the DME. The theory of multistep electrode reactions in dc polarography given by Ruzic^{9,14} is applicable to normal-pulse voltammetry. The current-potential relationship is

$$\frac{i}{i_d} = \frac{\frac{n_1}{n_1 + n_2} (K_c P^{n_2})^{1/(n_1+n_2)} + 1}{P + (K_c P^{n_2})^{1/(n_1+n_2)} + 1} \quad (6)$$

where

$$P = \exp \left[\frac{(n_1 + n_2)F}{RT} \left(\frac{E_1 + E_2}{2} - \frac{n_1}{n_1 + n_2} E_{1/2}^1 - \frac{n_2}{n_1 + n_2} E_{1/2}^2 \right) \right]$$

and i_d is given by the Cottrell expression:¹⁵ $nFA(D/\pi t)^{1/2}$ (see Appendix I for definitions). It is found that for $\Delta E_{1/2} < 200$ mV the steps are not cleanly resolved. Ruzic^{14,9a} noted this and suggested an analysis which requires recasting of experimental data into logarithmic form.

Differential Pulse. The technique of differential-pulse voltammetry at stationary electrodes has been studied by Keller and Osteryoung.¹⁰ Parry and Osteryoung¹⁶ theoretically and experimentally evaluated the effect of various experimental parameters on the resulting Δi vs. E curve. Their rather simple theoretical approach fits the experimental results closely.

Later, Keller and Osteryoung¹⁰ showed that a more rigorous derivation yielded a Δi vs. E relationship for stationary electrodes that reduces to the earlier result if D_O/D_R is assumed to be unity. Other authors have used digital simulation to evaluate the technique and obtain essentially the same results.¹⁷

The derivation of the pulse amplitude dependent current response given by Parry and Osteryoung¹⁶ has been criticized by some authors.^{18,19} However, Ruzic¹⁸ has shown that the Parry and Osteryoung result is correct and can be obtained from the original equations given by Barker and Gardner.²⁰

To obtain the relationship for Δi in the multistep case of eq 1, we begin with eq 6 and obtain the difference in current by subtracting i at E_1 from i at E_2 . The resulting expression is then rewritten in terms of

$$\sigma = \exp \left[\left(\frac{E_2 - E_1}{2} \right) \frac{(n_1 + n_2)F}{RT} \right]$$

where E_1 is the potential prior to the pulse and is the potential axis of the Δi vs. E curve recorded experimentally. The pulse amplitude is

$$E_{\text{pul}} = E_2 - E_1$$

We obtain

$$\frac{\Delta i}{i_d} = \left[\left(\frac{n_1}{n_1 + n_2} (K_c^{1/(n_1+n_2)}) (P\sigma)^{n_2/(n_1+n_2)} + 1 \right) / (P\sigma + (K_c^{1/(n_1+n_2)}) (P\sigma)^{n_2/(n_1+n_2)} + 1) \right] - \left[\left(\frac{n_1}{n_1 + n_2} (K_c^{1/(n_1+n_2)}) \left(\frac{P}{\sigma} \right)^{n_2/(n_1+n_2)} + 1 \right) / \left(\frac{P}{\sigma} + (K_c^{1/(n_1+n_2)}) \left(\frac{P}{\sigma} \right)^{n_2/(n_1+n_2)} + 1 \right) \right] \quad (7)$$

When $K_c = 4$, eq 7 reduces to the form of a single-step reaction as given by Parry and Osteryoung. When $E_{1/2}^1 - E_{1/2}^2$ is $\ll 0$, the curve approaches the shape of a multielectron wave with $n = n_1 + n_2$. Plots of the current function, eq 7, for Δi vs. E_1 at a 10-mV pulse amplitude are given in Figure 1 for various values of $\Delta E_{1/2}$.

It is apparent from Figure 1 that the theoretical differential-pulse curves have a form that is amenable to the construction of working curves. Since the most common situation involves $n_1 = n_2 = 1$, we have computed working curves for that case at $E_{\text{pul}} = 10$ mV. Two convenient parameters are the width at $\Delta i_{\text{max}}/2$ (or a composite if the waves are separated; see Appendix II) and the peak-to-peak separation (ΔE_p). For $K_c = 4$, the width is 90.9 mV as predicted from the equation of Parry and Osteryoung¹⁶ for a single step. As K_c increases from 4 ($\Delta E_{1/2} > 36$ mV), the curve broadens, and at $\Delta E_{1/2} \approx 75$ mV, two peaks become discernible. The composite or overall width at $\Delta i_{\text{max}}/2$ approaches the value $\Delta E_{1/2} + 90.9$ mV when $\Delta E_{1/2}$ becomes large. When $\Delta E_{1/2} > 160$ mV, the peak separation gives $\Delta E_{1/2}$ within about 1 mV.

Working curves for multistep DP voltammetry are given in Figure 2. In the region $\Delta E_{1/2} \geq 80$ mV, both curves can be used to obtain $\Delta E_{1/2}$. For accurate work, large-scale plots can

- (9) (a) Ruzic, I. *J. Electroanal. Chem.* **1974**, *52*, 1489. (b) Birke, R. L. *Anal. Chem.* **1978**, *50*, 1489.
 (10) Keller, H. E.; Osteryoung, R. A. *Anal. Chem.* **1971**, *43*, 342.
 (11) (a) Adams, R. "Electrochemistry at Solid Electrodes"; Marcel-Dekker: New York, 1969; p 280. (b) *Ibid.*, p 55.
 (12) Sawyer, D. T.; Roberts, I. L. "Experimental Electrochemistry for Chemists"; Wiley-Interscience: New York, 1974.
 (13) (a) Brinkman, A. A. M.; Los, J. M. *J. Electroanal. Chem.* **1964**, *7*, 171. (b) Fonds, A. W.; Brinkman, A. A. M.; Los, J. M. *Ibid.* **1967**, *14*, 43. (c) Oldham, K. B.; Parry, E. P. *Anal. Chem.* **1970**, *42*, 229.
 (14) Ruzic, I. *J. Electroanal. Chem.* **1970**, *25*, 144.
 (15) Reference 4, p 51.
 (16) Parry, E. P.; Osteryoung, R. A. *Anal. Chem.* **1965**, *37*, 1634.

- (17) Rifkin, S. C.; Evans, D. H. *Anal. Chem.* **1976**, *48*, 2174.
 (18) Ruzic, I.; Sluyters-Rehbach, M. *Anal. Chim. Acta* **1978**, *99*, 177.
 (19) (a) Heyne, G. S. M.; Van der Linden, W. E. *Anal. Chim. Acta* **1976**, *82*, 231. (b) Heyne, G. S. M.; Van der Linden, W. E. *Ibid.* **1978**, *99*, 183.
 (20) (a) Barker, G. C.; Gardner, A. W. Report C/R 2297; Atomic Energy Research Establishment: Harwell, 1958. (b) Barker, G. C.; Gardner, A. W. *Fresenius' Z. Anal. Chem.* **1960**, *173*, 79. (c) Gardner, G. C.; Faircloth, R. L.; Gardner, A. W. Report C/R 1786; Atomic Energy Research Establishment: Harwell, 1956.

Table I. Parameters for the Differential-Pulse Method^a

$\Delta E_{1/2}$, mV	$E_p^2 - E_{1/2}^1$, mV	$\Delta i_{\max}/i_d$	ΔE_p , mV	width, mV
300	-305	0.0485	299.8	390.9
250	-255	0.0485	249.8	341.0
200	-205	0.0486	199.6	291.2
180	-185	0.0487	179.4	271.2
160	-165	0.0489	159.0	250.7
140	-144	0.0494	138.0	230.0
130	-133	0.0498	126.8	219.2
120	-123	0.0504	115.4	208.5
110	-112	0.0514	103.0	197.2
100	-100	0.0529	89.0	185.6
90	-86	0.0552	72.6	172.8
80	-70	0.0591	50.4	158.6
70	-40	0.0659	0.8	141.6
60	-35	0.0746		124.2
50	-30	0.0837		107.8
40	-25	0.0929		95.8
35.61	-22.8	0.0970		90.9
30	-20	0.1023		85.4
20	-15	0.1115		77.2
10	-10	0.1205		70.9
0	-5	0.1290		65.9
-20	5	0.1443		59.0
-40	15	0.1569		54.6
-60	25	0.1668		51.7
-80	35	0.1743		49.8
-120	55	0.1836		47.8
-150	70	0.1873		47.0
-180	85	0.1895		46.5
-200	95	0.1904		46.3

^a Peak potential ($E_p^2 - E_{1/2}^1$), maximum current ($\Delta i_{\max}/i_d$), peak-to-peak separation (ΔE_p), and width for two-step differential pulse as a function of $\Delta E_{1/2}$. Data generated from eq 7 for various values of $\Delta E_{1/2}$. Pulse amplitude (E_{pul}) = 10 mV and $n_1 = n_2 = 1$. Symbols are defined in Appendix I. Parts of this table are used to construct working curves of Figure 4.

be constructed from the data in Table I. Theoretical data for pulse amplitudes other than 10 mV can be generated from eq 7 with programs available from the authors.

So that the actual values of $E_{1/2}^1$ and $E_{1/2}^2$ can be obtained, two cases are distinguished. For $\Delta E_{1/2} > 180$ mV, two peaks are clearly resolved and their E_p 's are related to the $E_{1/2}$'s (within 1 mV) by

$$E_p = E_{1/2} - \frac{E_{pul}}{2} \quad (8)$$

For any $\Delta E_{1/2}$, the center of symmetry of the curve, E_c (see Appendix II), is related to $E_{1/2}^1$ by

$$E_{1/2}^1 = E_c + \frac{\Delta E_{1/2} + E_{pul}}{2} \quad (9)$$

Cyclic Voltammetry. Since instruments for cyclic voltammetry are relatively simple¹¹ and more widely available than pulse instruments, we have extended the curves of Myers and Shain.⁷ This extension is possible if the parameter $E_p - E_{p/2}$ is defined as shown in Appendix II. The overall half-width of the initial scan (cathodic in the case of a reduction) vs. $\Delta E_{1/2}$ is shown in Figure 3. Data are provided in Table II to extend the treatment of Myers and Shain.⁷ The potential difference $E_p - E_{1/2}^1$ is tabulated in Table II and ref 7. This is the difference between the most cathodic peak (for a reduction) and $E_{1/2}^1$. In the limit of large $\Delta E_{1/2}$, this will be

$$E_p - E_{1/2}^1 = \left(E_{1/2}^2 - \frac{28.5}{n} \right) - E_{1/2}^1 \quad (10)$$

In addition, we have examined the use of the peak-to-peak separation in determining $\Delta E_{1/2}$. This parameter is the potential difference between the most cathodic peak and the most

Table II. Parameters for the Cyclic Voltammetric Method^a

$\Delta E_{1/2}$, mV	$E_p(\text{cathodic}) - E_{1/2}^1$, mV	i_p^b	ΔE_p , mV	$E_p - E_{p/2}$, mV
200	-225	0.639	252	236.3
160	-184	0.619	210	193.2
140	-164	0.674	188	172.7
120	-142	0.694	164	149.5
110	-131	0.706	152	137.7
100	-120	0.720	140	125.4
90	-107	0.739	126	113.1
80	-96	0.755	113	101.8
70	-84.0	0.779	98.9	89.7
60	-72.4	0.807	85.2	78.1
50	-61.1	0.838	72.4	68.3
40	-50.9	0.872	62.7	59.6
35.61	-46.7	0.892	58.5	57.0
30	-42.1	0.909	54.9	
20	-34.4	0.945	49.3	
10	-27.2	0.980	45.2	
0	-21.1	1.019	42.2	
-20	-8.3	1.078	37.0	
-40	2.5	1.124	37.9	
-60	13.2	1.162	34.0	
-100	34.8	1.212	30.8	
-200	85.4	1.254	29.8	

^a Peak potential ($E_p - E_{1/2}^1$), peak current (i_p), peak-to-peak difference (ΔE_p), half-width ($E_p - E_{p/2}$) of two-step cyclic wave as a function of $\Delta E_{1/2}$. See Appendix I for more detail on notation. The peak current (i_p) is defined in ref 8a. This table is used to construct the working curves of Figure 5. For this table, $n_1 = n_2 = 1$. ^b Current function defined in ref 6. ^c Continuation of the column found in ref 7.

anodic peak on the sweep after switching (see Appendix II). For $\Delta E_{1/2} < 120$ mV, only two peaks are resolved. The switching potentials for the simulations were chosen to occur at least 250 mV beyond $E_{1/2}^2$. Data are presented in Table II and working curves are shown in Figure 3.

Experimental Section

Electrochemistry. Normal- and differential-pulse voltammetry was done with a PAR Model 170 instrument, which has a 57-ms pulse width, with current sampled 40 ms after the pulse was applied. A sweep rate of 2 mV/s was used in all pulse experiments with a "drop time" of 0.5 s. Cyclic voltammetry was done with a PAR 173/176 potentiostat/programmer unit at a scan rate of 20 or 50 mV/s. All potentials were measured against a Beckman SCE reference.

The cell used in all experiments was an H-cell of the usual configuration, with the reference electrode chamber separated from the working solution by a fine glass frit. Electrolyte for all experiments was 1 M HCl. The auxiliary electrode was a platinum wire loop. A carbon-paste electrode¹¹ of approximately 0.07 cm² area was constructed from a Teflon sleeve and CP-O carbon paste (Bioanalytical, Inc.). The temperature for all experiments was 22 ± 1 °C. Working solutions millimolar in the polarizer were deaerated in the cell with prescrubbed argon.

Computations. Working curves for cyclic voltammetry were constructed from theoretical voltammograms obtained by the program of Polcyn and Shain.⁶ The "grid" was $\delta = 0.04$, which yields a 0.1% error in peak currents.^{6,8} Program listings for simulation of multistep pulse voltammetry (normal or differential) are available from the authors (Fortran IV). All computation was done at the Stanford University Center for Information Technology. Plotting was done with the local plotting routine TOPDRAWER.²¹

Synthesis. The preparation of the complexes $[(Ru(NH_3)_2L]X_4$ where L = 1,2-dicyanobenzene, 1,4-dicyanobenzene, 1,5-dicyanobenzene, and pyrimidine will be reported elsewhere ($X = CF_3SO_3^-$ or ClO_4^-).^{23a} The complex $[(Ru(NH_3)_2(4,4'-bpy)](ClO_4)_6$ was prepared by the procedure of Sutton.²

The compound $[Ru(NH_3)_2(\text{benzonitrile})](ClO_4)_2$, prepared by the method of Clarke and Ford,²² was used as a one-electron standard.

(21) Chaffee, R. B. Report CGTM 178; Computation Research Group, Stanford Linear Accelerator Center; Stanford, CA, 1978.

(22) Clarke, R. E.; Ford, P. C. *Inorg. Chem.* 1970, 9, 227.

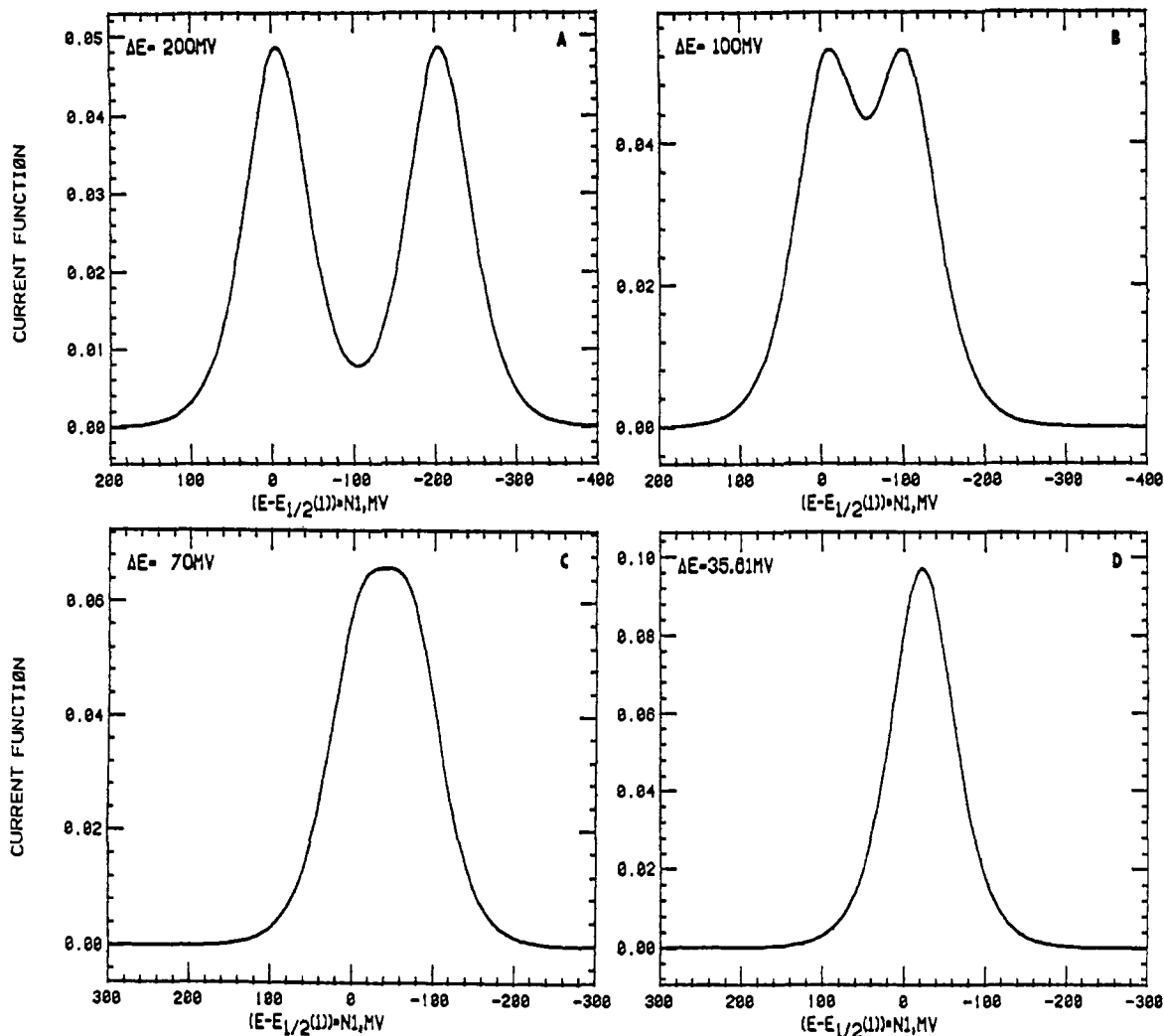


Figure 1. Theoretical current-potential curves for differential-pulse voltammetry (eq 7). The $\Delta E_{1/2}$ values are (A) 200, (B) 100, (C) 70, and (D) 35.61 mV. The current function is $\Delta i/i_d$, and the pulse amplitude is 10 mV.

Table III. Applications^a

bridge	ΔE_p^b	$E_p - E_{p/2}^b$	$E_{1/2}^1, E_{1/2}^2{}^c$	ΔE_p^d	width ^d	$E_{1/2}^1, E_{1/2}^2{}^e$
bipyridine	81 (23.4)	80 (22.5)	121, 41		79 (21.7)	125, 47
pyrimidine	150 (34.3)	150 (34.3)	286, 136	145 (283)	146 (294)	293, 147
1,2-dicyanobenzene	98 (45.4)	90 (33.2)	377, 287	85 (27.4)	88 (30.7)	376, 288
1,4-dicyanobenzene	82 (24.3)	81 (23.4)	340, 268		76 (19.3)	341, 265
1,5-dicyanonaphthalene	51 (7.3)	50 (7.0)	309, 259		50 (7.0)	314, 264

^a Results for the $[(NH_3)_5Ru\text{-bridge-Ru}(NH_3)_5]$ couples obtained by comparison of experimental cyclic and differential-pulse voltammetry data to the theoretical data of Tables I and II. Resulting values for $\Delta E_{1/2}$ (in mV) and K_c (in parentheses) are given. The half-potentials $E_{1/2}^1$ and $E_{1/2}^2$ (in mV vs. SCE) listed are obtained by application of eq 8 and 9 to the results of the width methods. ^b Cyclic voltammetry; mV. ^c From cyclic voltammetry width, $E_p - E_{p/2}$; mV. ^d Differential pulse voltammetry, mV. ^e From differential pulse width; mV.

The $[Ru(NH_3)_5NCC_5H_6]^{3+/2+}$ couple behaves reversibly at the carbon-paste electrode with no evidence of adsorption. Prior to each measurement of an unknown, this complex was run under identical conditions to confirm theoretically predicted behavior at the electrode. $E_{1/2}$ potentials from cyclic and differential-pulse methods generally agree within 2 mV for this one-electron standard.

Results

The five binuclear complex ions referred to in the preceding section were chosen to cover the range $\sim 4 < K_c < \sim 10^3$. Numerous other related binuclear complexes have been prepared, and further electrochemical and spectroscopic properties of all of these species will be reported elsewhere.^{23a} Elec-

trochemically determined values of $\Delta E_{1/2}$ and K_c are summarized in Table III. In general, good agreement (± 2 mV) was found between the $\Delta E_{1/2}$ values determined by the width methods of cyclic and pulse voltammetry. The peak-difference method of cyclic voltammetry often resulted in $\Delta E_{1/2}$ values as much as 10 mV different from the width methods. This is not unexpected, as will be discussed later. For the two examples where peak differences could be measured in differential pulse, good agreement was found with the width-method result. Individual cases are discussed below. Except for the bipyridine- and pyrimidine-bridged ions, all measurements were made on fully reduced samples. Therefore, the initial scan direction is anodic. For ease of comparison, cyclic voltammograms are shown with "inverted" potential axes, i.e., anodic scan toward the right.

(23) (a) Richardson, D. E.; Krentzien, H.; Taube, H., in preparation. (b) Krentzien, H. Ph.D. Thesis, Stanford University, 1979.

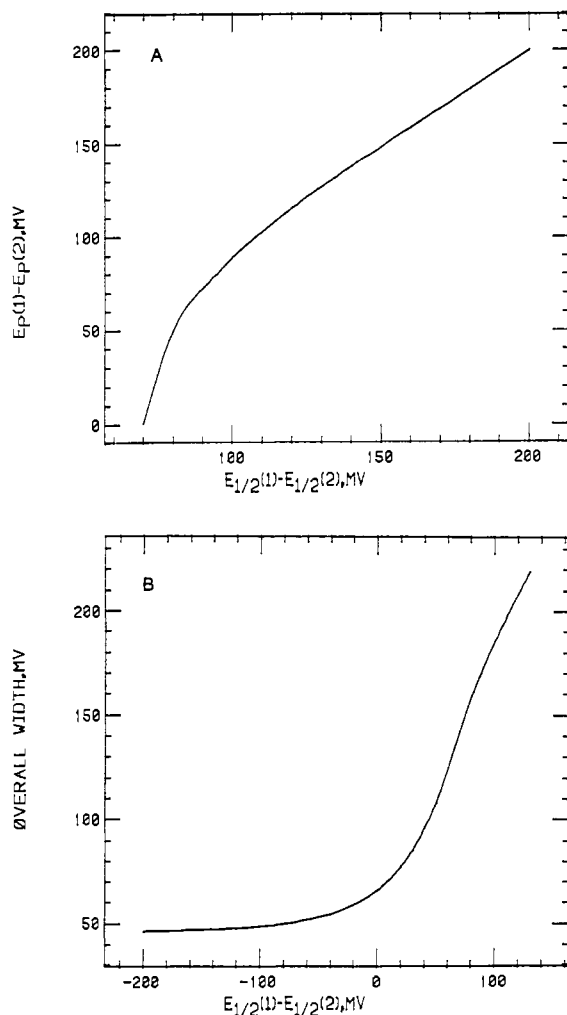


Figure 2. Working curve for multistep differential-pulse voltammetry ($n_1 = n_2 = 1$, $E_{\text{pul}} = 10$ mV): (A) ΔE_p vs. $\Delta E_{1/2}$; (B) width vs. $\Delta E_{1/2}$.

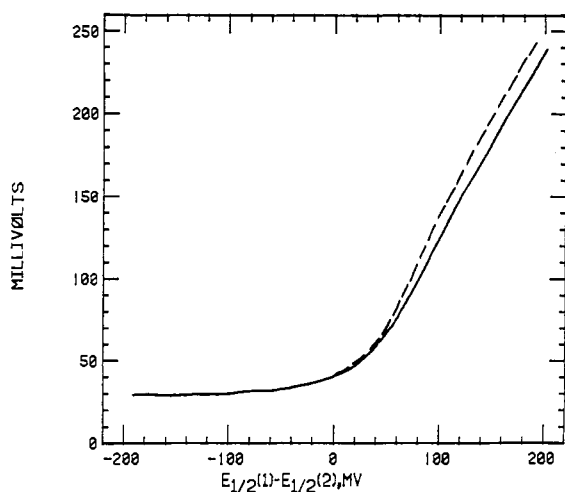


Figure 3. Working curve for multistep cyclic voltammetry: solid line, $E_p - E_{p/2}$ vs. $\Delta E_{1/2}$; dashed line, ΔE_p vs. $\Delta E_{1/2}$.

The 4,4'-bipyridyl-bridged binuclear complex was chosen to compare the results of the electrochemical methods with the spectroscopic titration technique. Sutton^{2b} reports K_c at 25 °C and $\mu = 1.0$ (HCl/NaCl) as 24. This is in fair agreement with the electrochemical results (average K_c by the width methods 22.1) in Table III. In Figure 4, we compare the theoretical and experimental current-potential curves with $E_{1/2}^1$ normalized to zero. The actual values of $E_{1/2}^1$ determined by the two width methods differ by 4 mV, which is

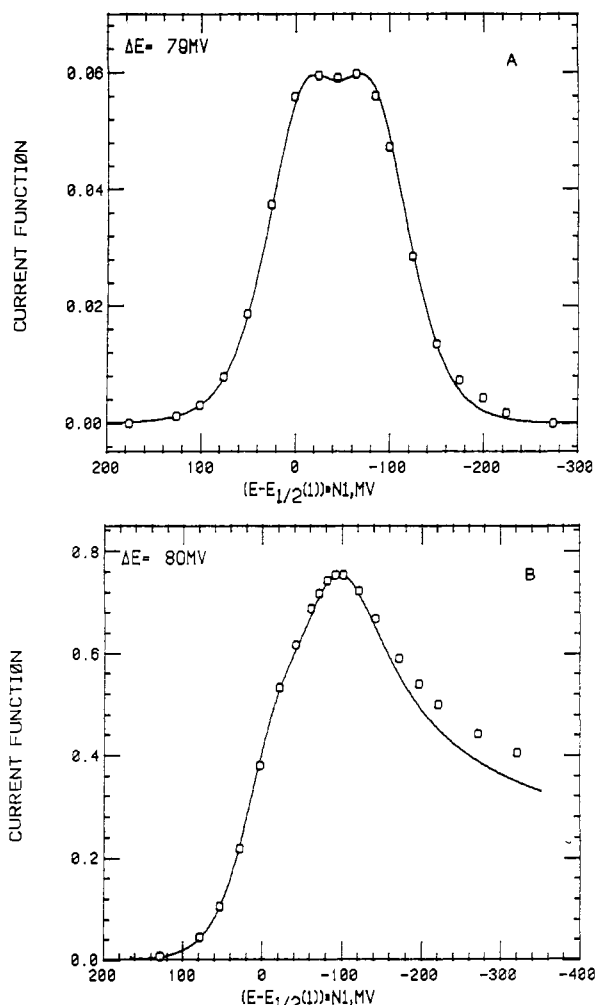


Figure 4. Comparison of experiment (O) to theory (—) for $[(\text{NH}_3)_2\text{Ru}]_2(4,4'\text{-bpy})^{4+/5+/6+}$ in 1 M HCl: (A) differential-pulse voltammetry ($E_{\text{pul}} = 10$ mV); (B) linear-sweep (single-scan) voltammetry. The potential scale is $(E - E_{1/2}^1)$. Actual $E_{1/2}^1$ values vs. SCE are given in Table III.

reasonable in view of the difficulty of locating accurate peak potentials (especially in cyclic voltammetry: see later discussion).

When pyrimidine is the bridging ligand, the width methods yield $K_c = 319 \pm 10\%$. The $E_{1/2}^1$ values from the two width methods agree within 6 mV. Graph-theoretical vs. experimental comparisons are shown in Figure 5.

In the case of the two isomers 1,2- and 1,4-dicyanobenzene, the results in Table III show that K_c is somewhat higher for the ortho isomer. From the width methods, $K_c(\text{ortho}) = 32$ and $K_c(\text{para}) = 21$ within about 10%.

For the 1,5-dicyanonaphthalene complex K_c approaches the statistical value of 4, not unexpected because of the large metal-metal distance (~ 12.4 Å from CPK molecules) and spectroscopic data that show the interaction to be weak.^{23a} Due to experimental uncertainties inherent in any electrochemical method, the observed K_c of 7 is probably within experimental error of 4. The differential-pulse width is 108 mV for $K_c = 7$, and the CV and DP curves are very much like a reversible one-electron couple in appearance.

Discussion

When a molecule contains multiple noninteracting sites, the relationship between the standard potential for each n -electron step and the number of sites per molecule is statistically determined. If the sites are noninteracting, it is reasonable to expect that current-potential response for a given electro-

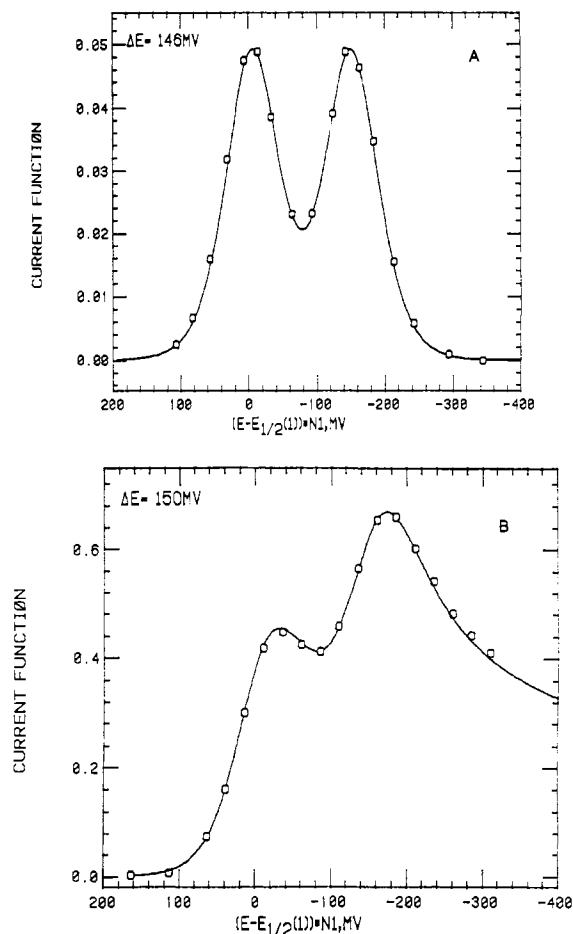


Figure 5. Comparison of experiment (O) to theory (—) for $[(\text{NH}_3)_5\text{Ru}]_2\text{pym}^{4+/5+/6+}$ in 1 M HCl. See Figure 4 caption for details.

chemical method will have the same form as a single-step charge transfer for a monomeric center. This result has been discussed extensively in a recent article by Flanagan et al.²⁴ For two noninteracting centers in one molecule, the difference in standard potentials is given by $(RT/nF) \ln 4$, or $35.61/n$ mV at 298 K. Therefore, when $\Delta E_{1/2} = 35.61/n$ for a two-step charge transfer involving n electrons per step, the cyclic and pulse responses studied here have the shape and current of a single-step charge transfer of $2n$ electrons.

With the exception of the 1,5-dicyanonaphthalene-bridged species, the values of K_c for the binuclear ions studied here are significantly higher than the statistical value of 4. Delineating the factors that contribute to a particular K_c is difficult, but trends can be found for the examples studied here. Some stability will arise from delocalization of the odd electron in the mixed-valence state, but this is not important in the cases studied here. More important is the electrostatic effect that favors the mixed-valence state. The relative importance of electrostatics is clearly illustrated in a comparison of the *o*- and *p*-dicyanobenzene-bridged binuclear ions. Both mixed-valence ions have an intervalence-transfer band in the near-infrared of roughly equal intensity, and on the basis of a simple Mulliken-type charge-transfer theory,^{2a,23a} the stabilities due to delocalization are about the same in the two cases. The metal-metal distances (6.8 Å for the ortho isomer, vs. 12.0 Å for the para) will cause the electrostatic effect to be greater in the ortho case. Table III shows that K_c is larger by ~ 100 cal/molecular unit for the ortho species. The quantity is about

that calculated from models of the electrostatic effect.^{23a,25}

For the pyrimidine (pym)-bridged ion $K_c \approx 3 \times 10^2$, equivalent to ~ 1300 cal/molecular unit. Since the intervalence band^{23a} for the mixed-valence species is weak ($f = 8 \times 10^{-4}$), the delocalization energy is negligible. It is unlikely that electrostatics can account for the relative stability of the mixed-valence ion (the metal-metal distance is 6.0 Å). Since the first oxidation of $[\text{Ru}^{\text{II}}\text{-pym-Ru}^{\text{III}}]^{4+}$ occurs within 10 mV of the monomeric complex $[\text{Ru}(\text{NH}_3)_5\text{pym}]^{2+}$, the binuclear species has no unusual instability. However, the shift in the MTL charge-transfer band indicates a substantial increase in the π -acid character of pym when bound to Ru(III). The oxidation of $[\text{Ru}^{\text{II}}\text{-pym-Ru}^{\text{III}}]^{5+}$ is therefore displaced to a higher potential. This electronic effect is operative in all the binuclear species studied here, but it is especially prominent in the pyrimidine case due to the small number of atoms in the bridge. Further examples and a more detailed discussion of these points will be presented elsewhere.^{23a,25}

Our experimental results (Table III) indicate that the width methods of cyclic and differential-pulse voltammetry give $\Delta E_{1/2}$ values that agree within about ± 3 mV. In the region of special interest ($\Delta E_{1/2} < 300$ mV), this gives K_c values with about a 10% variation. Assuming that experimental requirements for reversibility and diffusion are met, we estimate that the derived K_c 's are good to within 10%. Of course, this assumes that the correction of eq 4 is relatively small.

Cyclic Method. As shown by Nicholson and Shain,^{8a} the anodic peak potential for an initially cathodic cyclic sweep is dependent on the switching potential (E_s). Thus, the anodic peak potential will vary over several millivolts as E_s goes from 65 to 300 mV beyond $E_{1/2}$.^{8a} When E_s is greater than about 250 mV beyond $E_{1/2}$, the anodic peak comes within 1 mV of the "normal" $E_p - E_{1/2}$ of 28.5 mV. The cyclic simulations used here have a $(E_s - E_{1/2})/n$ of at least 250 mV in order to minimize the distortion of the anodic peak due to choice of E_s . Experimentally, such an arrangement may not be possible due to impurities, solvent breakdown, counterion interference, or other problems. For this reason, we prefer the single-scan method (first noted by Myers and Shain⁷) based on the width $E_p - E_{p/2}$. We have extended their calculations and confirmed the validity of the method experimentally.

A critical factor in determining $E_p - E_{p/2}$ from experimental data is the accuracy of the measured peak potential. The simulations show that the top 5% of the wave is approximately symmetric with respect to the peak, so simple graphical estimation is possible. The peak potential so measured will have an error of about ± 2 mV.

We have found that linear extrapolation of the data in Table I is a simple and accurate (± 0.5 mV) way to convert $E_p - E_{p/2}$ and ΔE_p to $\Delta E_{1/2}$. The values of $E_{1/2}$ for the two steps can be determined from the quantity $E_p - E_{1/2}^1$ obtained from Table I. For example, if $\Delta E_{1/2} = 50$ mV and $E_p = 100$ mV, then $E_{1/2}^1 = 100.0 + 61.1$ mV = 161 mV and $E_{1/2}^2 = 161 - 50$ mV = 111 mV.

Since Table I does not extend beyond $\Delta E_{1/2} = 200$ mV, a method for extracting $\Delta E_{1/2}$, $E_{1/2}^1$, and $E_{1/2}^2$ for those cases should be mentioned. Polcyn and Shain⁶ show that the descending branch of the stationary-electrode voltammogram can be expressed analytically. This branch can then be used as a base line for the second wave, and the resulting two waves can then be evaluated in the usual manner.^{8a}

At this point, we should correct a common misconception concerning the dependence of the cyclic current response on $\Delta E_{1/2}$. Considering two one-electron steps, it is often assumed that the observed current response is given by the direct sum of two one-electron responses separated by $\Delta E_{1/2}$. This method

(24) Flanagan, J. B.; Margel, S.; Bard, A. J.; Anson, F. C. *J. Am. Chem. Soc.* **1978**, *100*, 4248.

(25) Sutton, J. E.; Taube, H., in preparation.

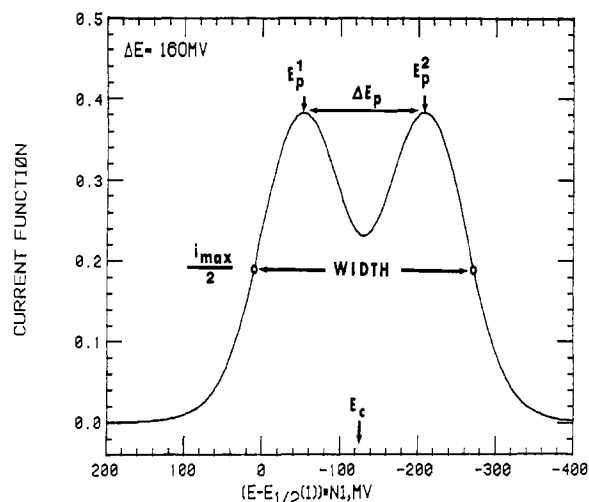


Figure 6. Definition of parameters for two-step differential-pulse voltammetry.

can only yield the correct response when $\Delta E_{1/2}$ is very large (so large that $E_{1/2}^1$ and $E_{1/2}^2$ can be measured directly, $\Delta E_{1/2} > 250$ mV). In the region of real concern, where the wave is distorted and direct measurement is impossible (e.g., Figure 2b of ref 6), the simple sum cannot possibly represent the correct response since at $\Delta E_{1/2} = 0$, $E_p - E_{p/2}$ would be 56.5 mV rather than the correct value of 41.5 mV.⁷ The sum method therefore has no theoretical basis and is not useful.

Differential Pulse. In contrast to the linear-sweep or cyclic method, the width method in differential-pulse voltammetry requires no measurement of peak potential; measurement of potentials at $\Delta i_{\max}/2$ is the only requirement. These potentials can be determined within about 1 mV. Again, we have found the linear extrapolation of the data in Table II is sufficiently accurate. Application of eq 8 or 9 will yield the actual $E_{1/2}$ for each step. For example, if $E_c = 100$ mV, $E_{\text{pul}} = 10$ mV, and $\Delta E_{1/2} = 50$ mV, then $E_{1/2}^1 = 100 + (50 + 10)/2$ mV = 130 mV and $E_{1/2}^2 = 130 - 50$ mV = 80 mV.

Our experimental Δi vs. E curves were symmetric with respect to E_c within 5% at $\Delta i_{\max}/2$. We should note that when more dilute electrolyte was used ($\mu = 0.1$), the curves for $\Delta E_{1/2} > 70$ mV became distinctly asymmetric. We did not examine the cause of this phenomenon closely but it is possibly due to migration effects at the stationary electrode.²⁶ Finally, we note that the differential-pulse method virtually eliminates charging-current interference,¹⁶ while the cyclic method can be experimentally complicated by a substantial charging current.

It should be noted that the DP response for a two-step charge transfer can be separated into two analytical curves only when $\Delta E_{1/2}$ approaches infinity in eq 7. As in the cyclic case, a simple sum of two n -electron responses cannot be used to determine $\Delta E_{1/2}$ except when $\Delta E_{1/2}$ is large. Practically, when $\Delta E_{1/2} \gtrsim 160$ mV, an error of < 1 mV will be introduced if the peak separation is used to measure $\Delta E_{1/2}$. In general, the methods discussed here have no simple relationship to the multicomponent techniques used to separate current responses arising from independent species with similar values of $E_{1/2}$.

Conclusion. Our extension of the cyclic method of Myers and Shain⁷ and the rather simple theory developed here for multistep differential-pulse Δi vs. E curves give two independent methods of determining $\Delta E_{1/2}$ for reversible two-step charge transfer. For kinetically stable species, the differen-

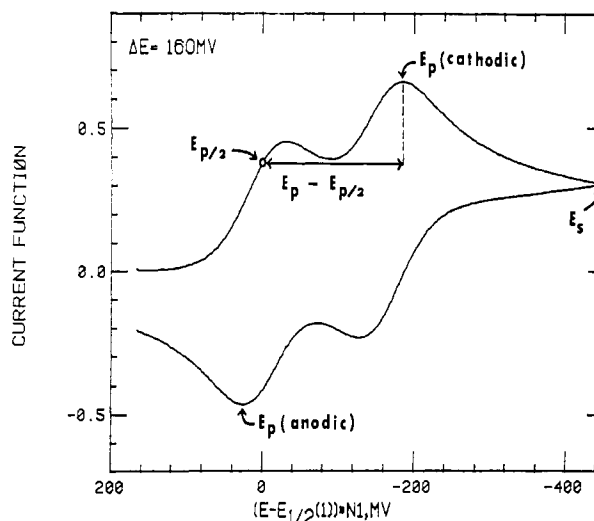


Figure 7. Definition of parameters for two-step cyclic voltammetry.

tial-pulse width method is preferred because of the accuracy of the measured width. For kinetically unstable species, the cyclic method can be used, providing the scan rate is not so large as to compete with the electron-transfer rate at the electrode.^{8b}

The agreement between the electrochemically and spectrophotometrically determined² K_c 's in the case of 4,4'-bipyridine as a bridging ligand is gratifying. On the basis of the limited comparison of theory and experiment given here, we would estimate that K_c can be determined within about 10% under ideal conditions.

It should be stressed that before the methods outlined here and those of Myers and Shain⁷ can be used, all other criteria must indicate that theoretical reversible behavior is observed at the electrode. A reversible standard of the type used here provides a check for working-electrode quality. It is also necessary that the current response for the unknown material be independent of scan rate in the region of the experimental cyclic scan rate. For both methods, it should be demonstrated that no chemical reactions complicate the observed Δi or i vs. E curves.

Acknowledgment. Support of this research by the National Science Foundation under Grant No. CHE76-09812-A2 is gratefully acknowledged. The authors thank Dr. Richard H. Holm for the use of the pulse electrochemical equipment and Dr. Daniel S. Polcyn for providing the cyclic voltammetry programs. Helpful discussions with Dr. Polcyn and Dr. Robert A. Osteryoung are gratefully acknowledged. The generous grant of computing time for dissertation research by the Stanford University CIT is acknowledged by D.E.R.

Appendix I. Notation

E_i°	standard potential of step i
$E_{1/2}^i$	half-reaction potential of step i (eq 4)
n_i	number of electrons in step i
K_c	comproportionation constant (eq 2)
D_O, D_R	diffusion coefficients for oxidized and reduced forms
f_O, f_R	activity coefficients for oxidized and reduced forms
C_X°	concentration of species X at the electrode surface
i_d	$nFA(D/\pi t)^{1/2}$ limiting current for linear diffusion
F	faraday constant
A	electrode area
i	measured current
Δi	measured current difference
E_{pul}	pulse amplitude
E_i	initial potential in normal-pulse voltammetry
E_s	switching potential in cyclic voltammetry

(26) (a) Heyrovsky, J.; Kuta, J. "Principles of Polarography"; Academic Press: New York, 1966; p 65. (b) Kolthoff, I. M.; Lingane, J. J. "Polarography"; Interscience: New York, 1952; Vol. 1, p 122.

Appendix II. Current-Potential Curve Parameters

The quantities of ΔE_p (peak-to-peak separation), E_c , and width used in the differential-pulse methods are defined in Figure 6.

In cyclic voltammetry (Figure 7), two quantities have been used. The width is given by $|E_p - E_{p/2}|$. The peak-to-peak separation is defined as

$$\Delta E_p = |E_p(\text{cathodic}) - E_p(\text{anodic})|$$

The absolute values are taken to allow application of the parameters to either initially cathodic (Figure 7) or initially anodic processes. $E_{p/2}$ is defined as the potential at which the current is half the peak current.

Registry No. $[(\text{NH}_3)_5\text{Ru}]_2(4,4'\text{-bpy})^{4+}$, 36451-88-4; $[(\text{NH}_3)_5\text{Ru}]_2\text{pym}^{4+}$, 76232-99-0; $[(\text{NH}_3)_5\text{Ru}]_2(1,2\text{-dicyanobenzene})^{4+}$, 76233-00-6; $[(\text{NH}_3)_5\text{Ru}]_2(1,4\text{-dicyanobenzene})^{4+}$, 76233-01-7; $[(\text{NH}_3)_5\text{Ru}]_2(1,5\text{-dicyanonaphthalene})^{4+}$, 76233-02-8.

Contribution from the Department of Chemistry,
Texas A&M University, College Station, Texas 77843

Reactions of Niobium(III) and Tantalum(III) Compounds with Acetylenes. 3.

Preparation and Structure of $[\text{TaCl}_2(\text{SC}_4\text{H}_8)(\text{Me}_3\text{CC}\equiv\text{CMe})]_2(\mu\text{-Cl})_2$

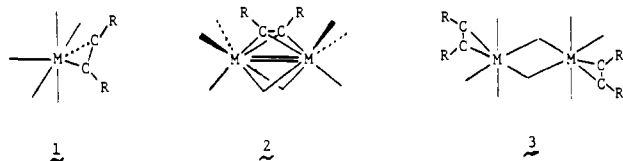
F. ALBERT COTTON* and WILLIAM T. HALL

Received April 11, 1980

The reaction of $\text{Ta}_2\text{Cl}_6(\text{SC}_4\text{H}_8)_3$ with $\text{CH}_3\text{C}\equiv\text{CCMe}_3$ gives rise to the binuclear compound $[(\text{CH}_3\text{CCMe}_3)(\text{SC}_4\text{H}_8)\text{Cl}_2\text{Ta}]_2(\mu\text{-Cl})_2$. We have isolated this compound and characterized it by X-ray crystallography. The crystals are monoclinic, and in space group $P2_1/n$ the unit cell parameters are $a = 10.952(9) \text{ \AA}$, $b = 11.716(4) \text{ \AA}$, $c = 13.097(6) \text{ \AA}$, $\beta = 107.45(5)^\circ$, $V = 1603(3) \text{ \AA}^3$, and $Z = 2$. Each molecule lies on a center of inversion and has a planar central $\text{Ta}(\mu\text{-Cl})_2\text{Ta}$ rhombus with $\text{Ta}-\text{Cl} = 2.496(3) \text{ \AA}$, $\text{Ta}-\text{Cl}' = 2.736(4) \text{ \AA}$, $\text{Cl}-\text{Ta}-\text{Cl} = 75.3(1)^\circ$, and $\text{Ta}-\text{Cl}-\text{Ta} = 104.7(1)^\circ$. The coordination sphere of each Ta atom is completed by two terminal Cl atoms (2.364(3) \AA), one sulfur atom (2.634(3) \AA), and the acetylene molecule, which is very strongly bonded, with $\text{Ta}-\text{C}$ distances of 2.03(1) \AA , a C-C distance of 1.32(2) \AA , and C-C \equiv C angles of 138(1) and 139(2)°.

Introduction

In several earlier communications¹⁻³ we have reported some results of our studies of the interaction of acetylenes with the niobium and tantalum compounds of the type $\text{M}_2\text{X}_6(\text{SC}_4\text{H}_8)_3$. Complexes which we have already described in detail are of types 1^{1,2} and 2,³ each of which has features of unusual interest.



We have now succeeded in characterizing structurally another stable alkyne complex which has still a different, but also novel and interesting, structure. Again our M^{III} starting material has been McCarley's $\text{Ta}_2\text{Cl}_6(\text{THT})_3$,⁴ where THT is a code for tetrahydrothiophene. As will be shown in the sequel, the new compound is of structural type 3.

Experimental Section

Synthesis and Crystal Preparation. Approximately 0.1 mL (~0.75 mmol) of *tert*-butylmethylacetylene (TMBA) was syringed into a flask containing 0.1 g (0.12 mmol) of $\text{Ta}_2\text{Cl}_6(\text{THT})_3$ (THT = tetrahydrothiophene) dissolved in 25 mL of toluene. This mixture was allowed to stand overnight at room temperature; a small amount of precipitate developed, and the solution was filtered into a separate flask. After 3 days, orange plate-shaped crystals formed on the walls of the vessel. These crystals were suitable for X-ray study, and the product was shown to be $\text{Ta}_2\text{Cl}_6(\text{THT})_2(\text{TMBA})_2$. The yield, on the basis of Ta starting material, was about 50%.

The compound decomposed within minutes on contact with air. All manipulations were performed under a nitrogen atmosphere, and toluene was distilled from sodium/benzophenone ketyl.

Table I. Atomic Positional Parameters for $\text{Ta}_2\text{Cl}_6(\text{CH}_3\text{CCMe}_3)_2(\text{SC}_4\text{H}_8)_2$

	x	y	z
Ta(1)	0.107 988	0.108 566	0.436 681
Cl(1)	0.019 998	0.070 695	0.608 406
Cl(2)	0.164 655	0.286 926	0.521 844
Cl(3)	0.285 795	0.000 575	0.537 463
S(1)	-0.118 905	0.202 665	0.355 170
C(1)	0.091 844	0.112 413	0.278 315
C(2)	0.207 875	0.146 821	0.332 964
C(11)	0.015 275	0.086 502	0.165 047
C(21)	0.325 252	0.190 889	0.309 943
C(22)	0.429 907	0.224 073	0.416 450
C(23)	0.374 057	0.097 644	0.249 319
C(24)	0.288 520	0.296 678	0.237 466
C(30)	-0.170 435	0.281 956	0.457 998
C(31)	-0.221 630	0.397 204	0.401 851
C(32)	-0.131 882	0.435 929	0.341 839
C(33)	-0.091 994	0.334 022	0.282 833

Data Collection and Structure Solution. A crystal was sealed in a capillary, in mineral oil, and mounted on a Syntex PI diffractometer. Preliminary photographic examination indicated that the crystals are monoclinic, and ω scans on several reflections showed the crystal selected to be of good quality. Systematic absences were consistent with space groups $P2_1/c$ or the equivalent alternate setting $P2_1/n$. The latter choice was made, and the following cell constants were obtained by centering on 15 intense reflections in the range $15^\circ < 2\theta < 28^\circ$: $a = 10.952(9) \text{ \AA}$, $b = 11.716(4) \text{ \AA}$, $c = 13.097(6) \text{ \AA}$, $\beta = 107.45(5)^\circ$, $V = 1603(3) \text{ \AA}^3$. For $Z = 2$ and a formula weight of 949.31, the calculated density is 1.966.

Data were collected at $20 \pm 2^\circ \text{ C}$, with use of molybdenum $K\alpha$ radiation. The θ - 2θ scan technique was employed with use of a variable scan rate of 4.0-24.0°/min with a scan range of 0.9° below $K\alpha_1$ to 0.9° above $K\alpha_2$. A total of 2182 reflections were collected in the range $0^\circ < 2\theta \leq 45^\circ$; 1942 of these had intensities greater than 3σ and were employed to solve and refine the structure. The intensities of three standard reflections, measured every 97 reflections, showed no change with time. Lorentz and polarization corrections were applied to the data, as was an empirical absorption correction based on ψ scans of four reflections near $\chi = 90^\circ$.

- (1) Cotton, F. A.; Hall, W. T. *J. Am. Chem. Soc.* **1979**, *101*, 5094.
- (2) Cotton, F. A.; Hall, W. T. *Inorg. Chem.* **1980**, *19*, 2352.
- (3) Cotton, F. A.; Hall, W. T. *Inorg. Chem.* **1980**, *19*, 2354.
- (4) Templeton, J. L.; McCarley, R. E. *Inorg. Chem.* **1978**, *17*, 2293.